Canadian Mineralogist
Vol. 21, pp. 101-113 (1983)

BEAVERITE – PLUMBOJAROSITE SOLID SOLUTIONS

J. L. JAMBOR AND J. E. DUTRIZAC
CANMET, 555 Booth Street, Ottawa, Ontario K1A 0G1

ABSTRACT

In synthetic plumbojarosite, incorporation of significant Cu or Zn (or both) increases with increasing concentrations of Cu^{2+} or Zn^{2+} in solution and, to a lesser extent, with increasing Pb/Fe^{3+} ratio. Replacement of Fe^{3+} by Zn^{2+} is minor, but the replacement by Cu^{2+} is sufficient to indicate that a compositional series probably extends from plumbojarosite $Pb[Fe_3(SO_4)_2(OH)_6]_2$ to beaverite $PbCuFe_2(SO_4)_2(OH)_6$. In the synthetic series, the atomic ratio Pb:(Cu + Zn) deviates from the expected value 1:1, and vacancies in *R* sites (involving Fe^{3+}, Cu^{2+}, Zn^{2+}) are common. Variations in cell parameters calculated from X-ray powder patterns show that *c* is related mainly to the amount of Cu^{2+} that has replaced Fe^{3+}; *a* is controlled principally by the proportions of Cu, Zn and Fe and the vacant *R* sites. Apparently significant deficiencies in alkali-site occupancy in jarosite may be partly compensated by hydronium substitution. Although most members of the jarosite group have $c \sim 17$ Å, an 11 Å diffraction line, in several specimens of synthetic and natural jarosite, which cannot be correlated with composition, suggests that some of the current concepts about the nature of jarosite are in need of fundamental revision.

Keywords: plumbojarosite, beaverite, osarizawaite, jarosite synthesis, (Fe, Cu) and (Fe, Zn) substitutions, composition of Pb-rich, jarosite, solid-solution series, plumbojarosite–beaverite.

SOMMAIRE

L'incorporation de Cu ou de Zn (ou des deux) en quantité notable dans la plumbojarosite synthétique augmente avec la concentration de Cu^{2+} ou de Zn^{2+} en solution et, à un degré moindre, avec l'augmentation du rapport Pb/Fe^{3+}. La substitution du zinc au fer est minime, mais celle du cuivre suffit à indiquer une solution solide continue, probablement sans lacune, de la plumbojarosite $Pb[Fe_3(SO_4)_2(OH_6]_2$ à la beaverite $PbCuFe_2(SO_4)(OH)_6$. Dans la série synthétique, le rapport Pb:(Cu + Zn) s'écarte du rapport prévu (1:1), et les lacunes parmi les sites *R* (Fe^{3+}, Cu^{2+}, Zn^{2+}) sont communes. La variation de la maille calculée à partir des spectres de poudre montre que *c* est principalement fonction de la substitution de Cu^{2+} à Fe^{3+}; *a* dépend surtout des rapports Cu: Zn: Fe et des lacunes dans les sites *R*. Des lacunes notables dans le site du métal alcalin dans la jarosite peuvent être partiellement compensées par substitution d'hydronium. Bien que les minéraux du groupe de la jarosite aient $c \sim 17$ Å, une raie de diffraction à 11 Å, observée dans plusieurs échantillons synthétiques et naturels, mais sans relation avec la composition, indique que certaines notions courantes sur la jarosite sont à réviser.

(Traduit par la Rédaction)

Mots-clés: plumbojarosite, beaverite, osarizawaite, synthèse de jarosite, substitution (Fe, Cu) et (Fe, Zn), solution solide plumbojarosite–beaverite.

INTRODUCTION

Metallurgical interest in beaverite $PbCuFe_2(SO_4)_2(OH)_6$ and copper–zinc-bearing synthetic plumbojarosite $Pb[Fe_3(SO_4)_2(OH)_6]_2$ has increased recently as a result of the recognition that these compounds are produced during the oxygen–sulfuric acid pressure leaching of Cu–Pb, Zn–Pb, or Cu–Zn–Pb sulfide concentrates (Scott 1973, Bolton *et al.* 1979). Synthetic plumbojarosite with a wide range of copper and zinc contents has been synthesized as part of an extensive CANMET investigation of the conditions of precipitation and the degree of solid solution that occur in the jarosite group (Dutrizac & Kaiman 1976, Dutrizac *et al.* 1980). Coincident with these syntheses, the first Canadian occurrence of beaverite was noted during a study of oxidized material from the Caribou massive-sulfide deposit, Bathurst area, New Brunswick (Jambor 1981). Identification of the Caribou beaverite was made by X-ray powder diffraction, and subsequently the composition of the mineral was verified by electron-microprobe analysis (Table 1).

Beaverite and most members of the jarosite group are reported to have a hexagonal unit cell with $a \sim 7$ Å and $c \sim 17$ Å; plumbojarosite and minamiite are exceptional in that their *c* dimensions are double those of the other minerals of the group. Despite this distinction, ambiguities arose in the X-ray powder identification of synthetic compounds compositionally equivalent to cuprian plumbojarosite. Therefore, the synthetic series, as well as some natural

specimens, were studied in more detail, as reported herein.

Structural and Solid-Solution Aspects

The structures of alunite and the jarosites were determined by Hendricks (1937) and have been refined by Menchetti & Sabelli (1976), Kato & Miura (1977) and Wang *et al.* (1965). In simplified terms, the structure is sheetlike in that the trivalent ions (Fe,Al) form R^{3+}(O,OH) octahedra that are corner-linked in a plane parallel to (0001). The octahedral layers are stacked along *c* in such a way as to enclose a large site in which a 12-co-ordination cation such as K^+, Na^+ or Pb^{2+} can be accommodated. Thus, substitution among the trivalent ions such as Al and Fe affects mainly the *a* dimension, whereas substitution for the 12-co-ordination cation mainly affects the *c* dimension.

In the case of plumbojarosite, the general jarosite formula $A^+R^{3+}{}_3(SO_4)_2(OH)_6$ requires modification because the A^+ sites are occupied by divalent lead. In the initial structural study of plumbojarosite (Hendricks 1937), it was concluded that charge balance is attained because only half of the A^+ sites are filled by Pb^{2+}; the *c* axis is doubled and the formula becomes $Pb[Fe_3(SO_4)_2(OH_6)]_2$. In beaverite, according to Palache *et al.* (1951), charge balance is attained by substitution of Cu^{2+} in the R^{3+} position: $Pb(Cu,Fe,Al)_3(SO_4)_2(OH)_6$. As the *c* axis is not doubled in beaverite, it is evident that the Pb:Cu ratio must be maintained at 1:1 to retain charge balance if other compensatory substitutions have not occurred. Analyses of type beaverite from Utah (Butler & Schaller 1911) and of beaverite from other occurrences (Bolgov 1956, Vitovskaya 1960, Enikeev 1964, Van Tassel 1958, Taguchi *et al.* 1972) all show Pb:Cu close to 1:1. However, in the synthetic series studied herein, Cu is variable and does not maintain the 1:1 ratio with Pb.

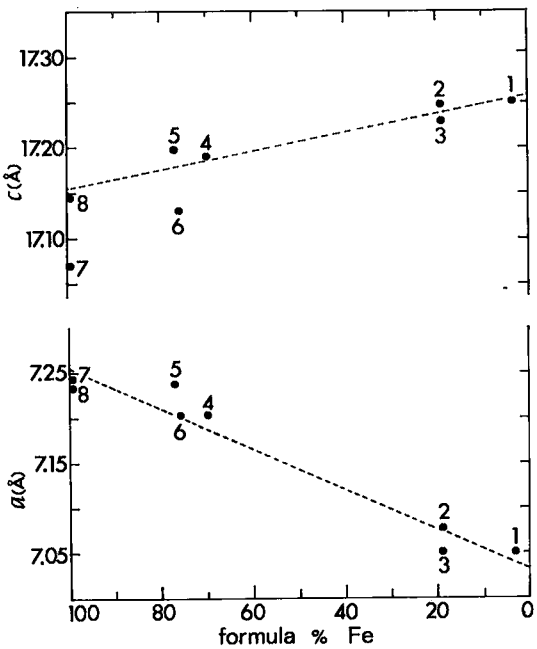

FIG. 1. Variations in *a* and *c* for osarizawaite: (1) after Morris (1963), (2) Giuseppetti & Tadini (1980), (3) Taguchi (1961). Beaverite: (4) after Taguchi *et al.* (1972), (5) Pabst (in Morris 1962), (6) revised PDF 17–476, (7) Caribou deposit, New Brunswick, and (8) Katanga (BM 1949–61).

Aside from the presence of Cu in beaverite, there is commonly some substitution of Al^{3+} for Fe^{3+}. Brophy *et al.* (1962) have shown that there is complete Al–Fe solid solution between alunite and jarosite; this observation has relevance in that the crystal structure of osarizawaite, the aluminum analogue of beaverite, was determined recently by Giuseppetti & Tadini (1980) and was shown to have $a \sim 7$ Å, $c \sim 17$ Å. Therefore, it can be assumed that beaverite has similar cell dimensions, and that solid solution between beaverite ($c \sim 17$ Å) and plumbojarosite ($c \sim 34$ Å) is either incomplete or involves a structural discontinuity. The initial problem was to establish accurate cell-parameters for beaverite and plumbojarosite so that the synthetic series could be related to these end members.

Beaverite – osarizawaite

Cell dimensions of osarizawaite and beaverite are shown in Figure 1. Data points for osarizawaite are from Morris (1962, 1963) and Taguchi

TABLE 1. MICROPROBE ANALYSES AND CELL DIMENSIONS OF BEAVERITE

		Caribou, New Brunswick	Katanga (BM 1949-61)	Theoretical
wt.%	PbO	31.4	34.0	32.98
	CuO	11.6	11.9	11.76
	Fe_2O_3	21.3	22.7	23.61
	SO_3	22.2	24.0	23.67
		86.5	92.6	92.02
		ratios for SO_4 = 2		
	Pb	1.02	1.02	1.00
	Cu	1.05	1.00	1.00
	Fe	1.92	1.90	2.00
	a(Å)	7.234(4)	7.243(2)	
	c(Å)	17.14(1)	17.14(1)	

Analyses by T.T. Chen. Al, Ag, Zn, K, Na not detected.
Synthetic $PbSO_4$, Cu_2O, Fe_2O_3 used as standards.

(1961). The composition of the osarizawaite used by Giuseppetti & Tadini (1980) is not known, but their description suggests that the crystal is part of the material that was studied by Taguchi (1961).

Data for aluminum-rich beaverite are from Taguchi *et al.* (1972) and from PDF 17–476, the latter giving cell dimensions of *a* 7.20, *c* 16.94 Å. As a *c* axis of 16.94 Å seemed too small, the new value shown on Figure 1 was obtained by least-squares refinement of the observed *d*-values using 15 lines from 3.60 to 1.52 Å. A similar refinement was used for the X-ray data of Pabst (in Morris 1962).

The two specimens of end-member beaverite are from the Caribou deposit, New Brunswick, and from Katanga, now Shaba, Zaire [BM 1949–61, British Museum (Natural History)]. Microprobe analyses of both specimens (Table 1) indicate that they are Al-free and have Pb:Cu close to 1:1. A third specimen, from Beaver County, Utah (Royal Ontario Museum, M8771) was not used because it was found by electron-microprobe analysis to contain 2.1 wt.% arsenic.

The results from the powder-diffraction data show that *a* expands from about 7.03 Å for osarizawaite to about 7.25 Å for the beaverite end-member. The variation is represented by the equation a (Å) = 7.0338 + 0.002204 Fe, where Fe is the formula % Fe (Fig. 1); the standard deviation in *a* is 0.02148. As both beaverite and osarizawaite have only ⅔ of their R^{3+} sites affected by the (Al, Fe) substitution, the other third being occupied by Cu, the change in *a* is similar to the 0.32 Å expansion from alunite to jarosite that was established by Brophy *et al.* (1962).

Although substitutions in the R^{3+} sites affect mainly the *a* dimension, Brophy *et al.* (1962) noted a slight decrease of ~0.09 Å in *c* from alunite $KAl_3(SO_4)_2(OH)_6$ to jarosite $KFe_3(SO_4)_2(OH)_6$ despite the larger radius of Fe^{3+} compared with that of Al^{3+}. A decrease in *c* also occurs from osarizawaite to beaverite; it is represented by c (Å) = 17.2556 – 0.00103 Fe, where Fe is the formula % Fe (Fig. 1); the standard deviation in *c* is 0.02308.

Plumbojarosite

A least-squares refinement of the X-ray powder pattern of synthetic plumbojarosite prepared in this study gave *a* 7.319(4), *c* 33.78(2) Å; plumbojarosite from the type locality has *a* 7.315, *c* 33.758 Å (Mumme & Scott 1966; PDF 18–698). Although these cell values are accepted as the end points, it should be noted that Kato (1979) reported *a* 7.305(2) and *c* 33.564(4) Å for a crystal of plumbojarosite from the Tintic Standard mine, Utah.

Synthetic Copper- and Zinc-Bearing Lead Jarosite

Syntheses

Reagent-grade chemicals were used for all syntheses. The plumbojarosite compositions were prepared by reacting an excess of solid $PbSO_4$ with solutions containing ferric sulfate plus various amounts of copper sulfate (± zinc sulfate) in an autoclave at 130°C for 24 hours. Optimum operating conditions were attained by reacting a twofold excess of $PbSO_4$ in a well-stirred baffled reactor containing 1 litre of 0.3 *M* Fe^{3+} as $Fe_2(SO_4)_3$ and 0.03 *M* H_2SO_4. The optimum operating conditions and the effects of acid and iron concentrations are discussed in Dutrizac *et al.* (1980).

Excess $PbSO_4$ was selectively leached from the jarosite precipitate by washing with four 1-litre portions of 10% ammonium acetate solu-

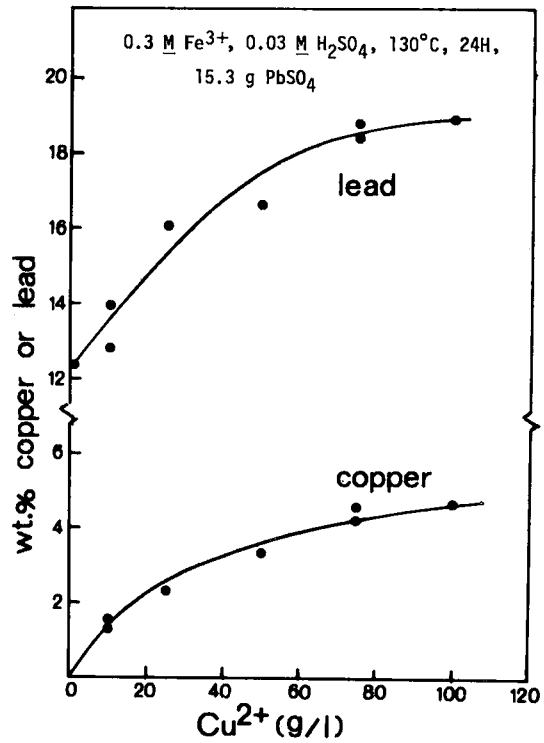

FIG. 2. The effect of dissolved copper concentration on the copper and lead contents of synthetic jarosite.

tion at 25°C. The jarosite residue was then filtered, water-washed, and dried at 110°C prior to chemical analysis and X-ray diffraction study. All samples of synthetic jarosite were checked for residual $PbSO_4$ by Guinier X-ray patterns; separate experiments established that as little as 0.3 wt.% $PbSO_4$ was faintly detectable on the Guinier patterns.

Figure 2 shows the effect of the Cu^{2+} ion concentration (as $CuSO_4$) on the copper and lead contents of the jarosite product. Higher copper concentrations in solution result in an increased copper uptake in jarosite; the effect is most pronounced for low additions of Cu^{2+}, and the curve flattens at 100 g/L Cu^{2+}. Significantly, the lead content of the jarosite also increases, suggesting that there has been a compensating incorporation of *A*-site Pb^{2+} accompanying the *R*-site (Cu^{2+},Fe^{3+}) substitution.

Figure 3 shows the effect of the $PbSO_4/Fe^{3+}$ molar ratio on the copper and lead contents of jarosite made from 0.3 *M* Fe^{3+} –0.03 *M* H_2SO_4 solutions containing 100 g/L Cu^{2+} as $CuSO_4$. For these conditions the stoichiometric amount of $PbSO_4$ is 15.3 g. Based on this and previous studies (Dutrizac *et al.* 1980, Dutrizac & Dinardo 1982), it has been found that increasing the stoichiometric ratio $PbSO_4/Fe^{3+}$ increases both the copper and lead contents of the products, with the effect most pronounced for $PbSO_4/Fe^{3+}$ ratios less than 2.

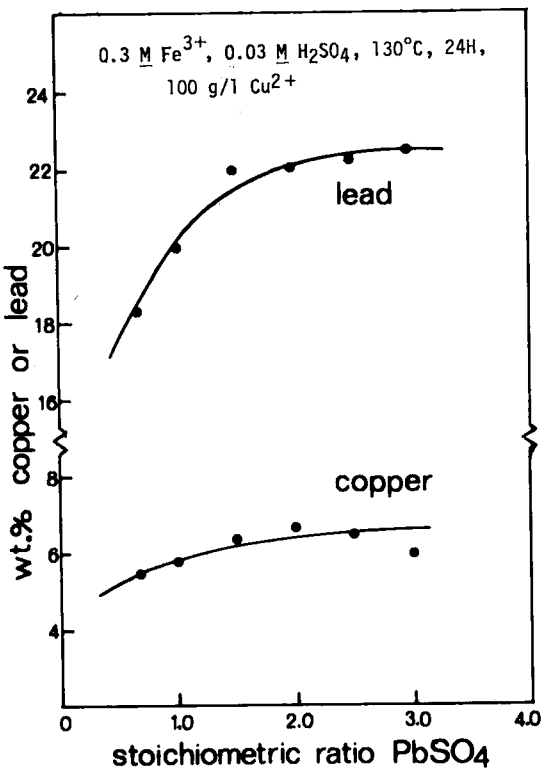

FIG. 3. Influence of the stoichiometric ratio of $PbSO_4$ on the lead and copper contents of synthetic jarosite.

In addition to syntheses involving Cu substitution in plumbojarosite, the same procedures were used to determine Zn uptake, both in the presence and absence of Cu. The behavior of Zn was found to be similar to that of Cu, but Zn substitution in the synthetic plumbojarosite is limited to a maximum of only about 4 wt.%. With both Cu and Zn in the aqueous solution, Zn incorporation is substantially depressed (to about 1 wt.% max.), and Cu uptake is slightly enhanced. Experimental results indicate that there is a significant preferential incorporation of Cu over Zn in synthetic plumbojarosite (Dutrizac & Dinardo 1982).

Results of analyses

Results of the chemical analyses of the synthetic plumbojarosites are given in Table 2. Plumbojarosite D2091, which was prepared in the same way as the Zn- and Cu-bearing series, shows a substantial deficiency in Pb^{2+} and Fe^{3+} relative to sulfate and the theoretical formula. Indeed, many samples of natural and synthetic jarosite in this and other studies are nonstoichiometric and iron- and alkali-deficient, though usually the latter is accompanied by an excess of formula water that probably represents hydronium (Kubisz 1970, Dutrizac & Kaiman 1976). The solid-solution series established by Mumme & Scott (1966) for plumbojarosite and basic ferric sulfate undoubtedly represents plumbo-jarosite – hydronium jarosite: $Pb[Fe_3(SO_4)_2(OH)_6]_2$ – $(H_3O)_2[Fe_3(SO_4)_2(OH)_6]_2$. In the present study, the total water obtained both by difference and by TGA also is consistently high and exceeds the amount of (OH) necesasry to maintain charge balance with the cations (Table 2). The excess water may be present as hydronium ion, a possibility that remains unresolved because there is no simple method for a direct quantitative determination of hydrodium. An attempt to resolve this aspect of jarosite composition is being pursued by laser Raman spectroscopy and low-temperature infrared absorption spectroscopy. Mössbauer studies have confirmed that all the iron in the samples of synthetic jarosite is in the ferric state (Leclerc 1980).

TABLE 2. CHEMICAL ANALYSES AND FORMULA RATIOS OF SYNTHETIC JAROSITES

	D2091	D2090	J288	J289	J290	J281B	J282B	J283	J326	J308	J309	J310	J311	J335	beaverite	plumbo-jarosite
PbO	10.54	12.76	17.68	19.61	20.01	15.10	17.43	18.05	23.82	20.36	19.16	21.17	22.89	25.35	32.98	19.74
CuO	-	-	-	-	-	1.93	3.42	4.42	8.36	4.56	5.51	6.74	7.39	8.29	11.76	-
ZnO	-	1.05	3.11	3.74	4.77	-	-	-	-	1.03	0.71	0.54	0.47	0.30	-	-
Fe_2O_3	44.12	42.77	38.74	36.92	36.16	39.75	38.30	36.68	30.72	34.98	36.32	34.32	33.09	28.96	23.61	42.37
SO_3	31.31	30.69	28.24	27.31	27.59	29.64	29.01	28.46	26.34	28.11	27.49	26.81	26.76	25.47	23.67	28.33
Total	85.97	87.27	87.77	87.58	88.53	86.42	88.16	87.61	89.24	89.04	89.19	89.58	90.60	88.37	92.02	91.44
Rem.*	14.03	12.73	12.23	12.42	11.47	13.58	11.84	12.39	10.76	10.96	10.81	10.42	9.90	11.63	7.98	9.56
TGA**	13.36	12.23	10.70	10.22	10.05	11.17	10.97	11.04	10.05	10.12	10.92	10.16	9.96	9.95		
							formula contents for $SO_4 = 2$									
Pb	0.242	0.298	0.450	0.555	0.561	0.366	0.431	0.455	0.649	0.520	0.500	0.567	0.614	0.714	1.000	0.500
Cu	-	-	-	-	-	0.131	0.237	0.297	0.639	0.326	0.403	0.506	0.555	0.655	1.000	-
Zn	-	0.067	0.217	0.269	0.340	-	-	-	-	0.072	0.051	0.039	0.035	0.023	-	-
Fe	2.825	2.794	2.750	2.711	2.628	2.689	2.646	2.584	2.338	2.495	2.650	2.566	2.479	2.280	2.000	3.000
$(OH)_t$	7.64	6.04	6.79	6.71	6.53	6.75	6.78	6.95	6.84	6.45	7.12	6.79	6.67	7.00		
$(OH)_r$	4.96	5.11	5.58	5.78	5.69	5.06	5.58	5.26	5.59	5.32	5.86	5.92	5.84	5.58	6.00	6.00
$a(\mathring{A})$	7.319(4)	7.323(3)	7.327(4)	7.324(3)	7.326(3)	7.307(4)	7.300(3)	7.294(3)	7.277(4)	7.294(3)	7.292(3)	7.288(3)	7.276(3)	7.278(4)		
$c(\mathring{A})$	33.78(2)	33.75(2)	33.76(2)	33.76(2)	33.73(3)	33.79(2)	33.86(2)	33.88(2)	34.00(2)	33.88(2)	33.92(2)	33.96(2)	33.97(2)	34.01(3)		
$I_{11\mathring{A}}$†	absent	medium	weak	faint(?)	absent	weak	faint(?)	faint	absent	absent	v. faint	absent	absent	v. weak		

* Rem. is the analytical total subtracted from 100 wt%
$(OH)_r$: amount of (OH) required to achieve charge balance in the formula
$(OH)_t$: amount of (OH) calculated from thermogravimetric analysis

** Weight loss by thermogravimetric analysis; H_2O evolved on heating 450°C.
†: intensity of the 11Å powder-diffraction line

Cation relations among synthetic members

Figure 4 shows the compositional variations for assumed solid solutions among beaverite, plumbojarosite and hydronium jarosite. The cations of concern are $(H_3O)^+$, Pb^{2+}, Cu^{2+} and Fe^{3+} which, in each mineral, are combined for a total charge of +10. The anions are shown only for the end members but in all cases are $2(SO_4)^{2-}$ and $6(OH)^-$ for a total charge of −10. The *R* sites are filled completely, and thus all sites vacated by Fe^{3+} are occupied by Cu^{2+}. Intermediate compositions along the plumbojarosite – beaverite join have Pb > Cu, whereas those along the join beaverite – hydronium jarosite have Pb = Cu. Occupancy of *A* sites ranges from 1.0 to 0.5, with the latter represented only by plumbojarosite (Fig. 4).

Figure 5, which represents the same composition field as Figure 4, shows the compositions of synthetic jarosite plotted solely on the basis of their Fe^{3+} *versus* Pb^{2+} formula ratios (Table 2). Data points for the synthetic copper–lead series (solid dots in Fig. 5) fall close to the join between hydronium jarosite and beaverite. Similarly, as none of the data points falls along the beaverite – plumbojarosite join, one must infer from the Pb^{2+}:Fe^{3+} ratios that all the samples of synthetic jarosite contain substantial amounts of hydronium ion. Note, however, that compositions along the join hydronium jarosite – beaverite progressively decrease in H_3O toward beaverite, and that the Pb:Cu ratio is constant at 1:1. These relations are not present in the samples of synthetic jarosite (Table 2).

Figures 6 and 7 show that increases in Pb^{2+} and decreases in Fe^{3+} accompany the substitution of divalent ions for Fe^{3+} in synthetic jarosite. Also evident in Figure 6 is an apparent break in the trend of the data points where Cu +Zn is in the range 0.3–0.5. Above this range, Pb:(Cu + Zn) ratios approximate 1:1 as in beaverite, whereas below this range Pb:(Cu + Zn) exceeds 1:1 as might be expected for cuprian or zincian plumbojarosite.

X-Ray Powder Study

X-ray powder patterns of natural beaverite and the synthetic lead-bearing jarosite series were obtained with 114.6-mm-diameter Debye–Scherrer cameras using filtered Co$K\alpha$ radiation ($\lambda = 1.7889$ Å). Measured 2θ values were corrected for film shrinkage using back reflections. A minimum of 13 clearly resolved and unambiguously indexed diffraction-lines, each assigned an equal weight, were used in the least-squares refinements to obtain the cell dimensions. Indexing of the patterns was done by using, as starting points, PDF 18–698 (natural plumbojarosite) and data in Dutrizac & Kaiman (1976) for synthetic plumbojarosite. Most diffraction lines have unique indices, but in some cases, alternative indices are possible for jarosite of a specific composition; therefore, selection of indices was done only after monitoring changes throughout the synthetic series. A representative pattern of ferrian beaverite and the *hkl* assignments used throughout the series are given in Table 3. For reasons that will be discussed below, all samples of synthetic jarosite were indexed using the doubled (~34 Å) *c* axis that characterizes plumbojarosite.

Composition versus cell dimensions

Giuseppetti & Tadini (1980) concluded from

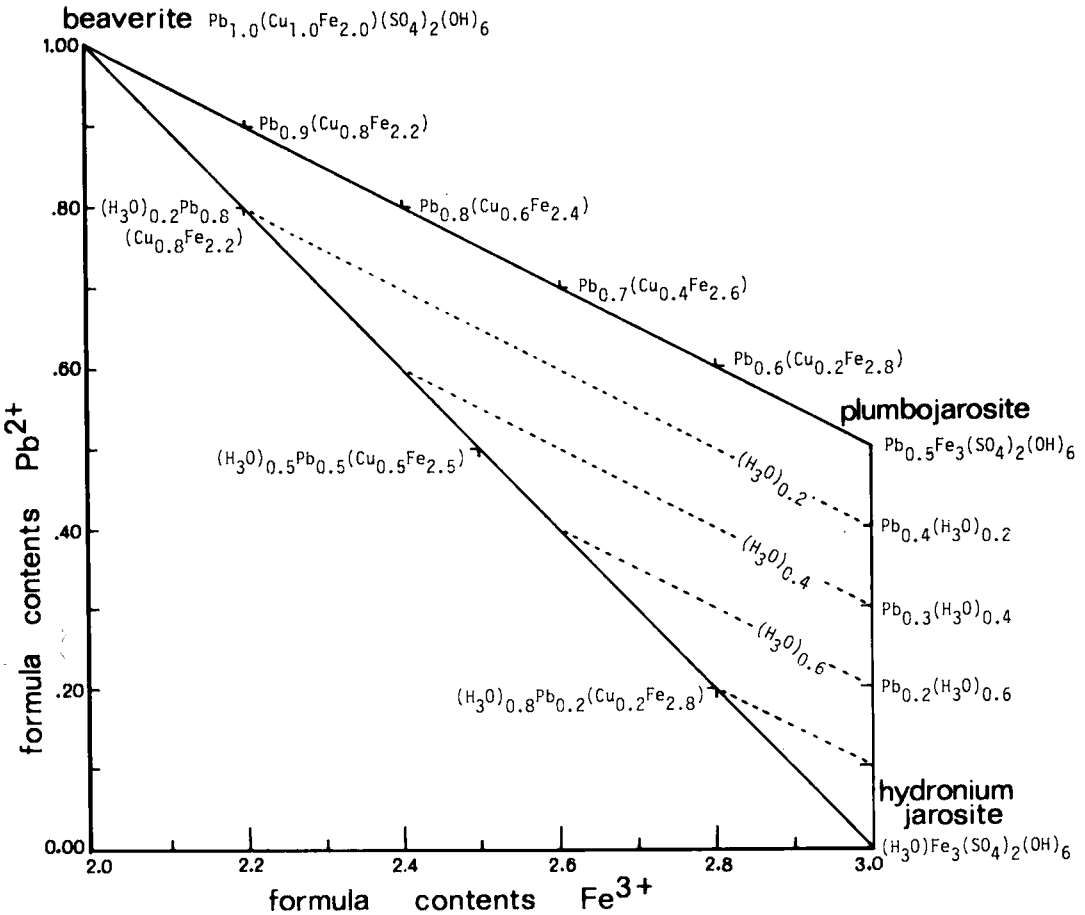

FIG. 4. Compositional variations for hypothetical solid solution among beaverite, plumbojarosite and hydronium jarosite assuming $(SO_4)_2$ and $(OH)_6$.

their structural study of osarizawaite that Al^{3+}, Fe^{3+} and Cu^{2+} are in random occupancy in *R* sites and that a replacement of Fe^{3+} ($r = 0.67$ Å) and Al^{3+} ($r = 0.50$ Å by Cu^{2+} ($r = 0.83$ Å) should expand the sheet-like jarosite structure mainly along *a*. However, the length of *c* was inferred to remain relatively constant because expansion along *a* permits greater interpenetration of neighboring sheets, thus reducing the amount of increase otherwise expected.

Figure 8 shows the variation in *a* and *c* for beaverite, plumbojarosite and the samples of synthetic jarosite. Synthetic jarosite with Zn^{2+} ($r = 0.74$ Å) as the only divalent ion in *R* has *c* similar or slightly smaller, and *a* consistently larger than the dimensions of end-member plumbojarosite. In contrast, the samples of synthetic copper-bearing jarosite have *a* and *c* on trends toward beaverite. Thus, although Cu and Zn are divalent ions of similar size, their effects on the cell parameters are distinctly different. For jarosite compositions without Cu, the effect of Zn on *a* is described by the regression equation *a* (Å) = 7.3184 + 0.02581 Zn, where Zn is the formula content of Zn as shown in Figure 8; the standard deviation in *a* is 0.00284. Similarly, the equation for *c* (Å) is 33.7669 − 0.07123 Zn, and the standard deviation in *c* is 0.01398. For Cu-bearing jarosite compositions, in which the formula content of Zn is less than 0.07, the equations for the lines shown in Figure 8 are *a* (Å)= 7.3208 − 0.07483 (Cu + Zn), and *c* (Å) = 33.7227 + 0.51209 (Cu +Zn); standard deviations are 0.00589 in *a* and 0.04891 in *c*.

The synthetic jarosite samples demonstrate that it is possible to have members of intermediate composition between plumbojarosite

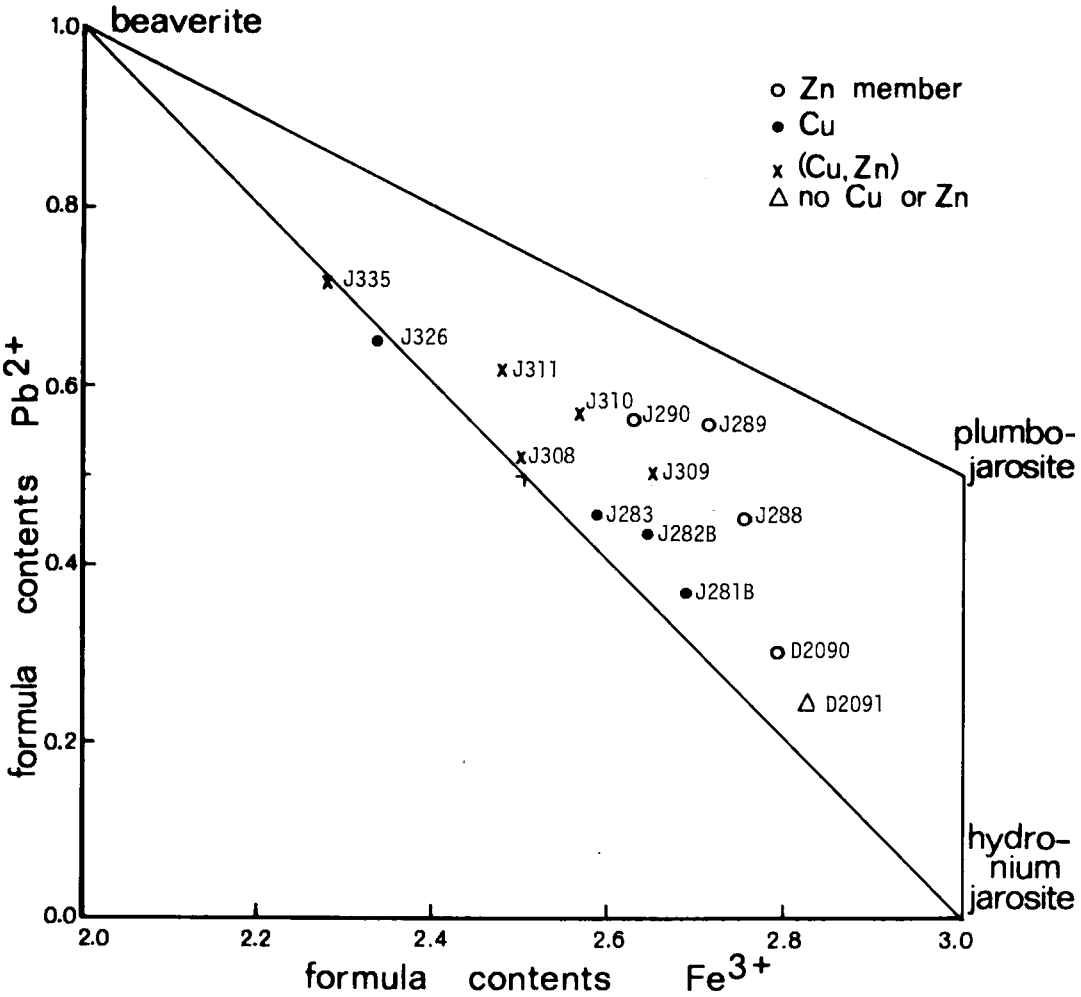

FIG. 5. Reference numbers and positions of the samples of synthetic jarosite plotted according to their Pb^{2+} *versus* Fe^{3+} formula contents as given in Table 2.

and beaverite. Cell dimensions of the synthetic samples would be expected to fall exactly on those for the beaverite – plumbojarosite join only if the formula range for Pb were 0.5 to 1.0, Cu + Fe = 3, and H_2O = OH. The results of the chemical analyses indicate that the synthetic jarosite compositions do not meet these constraints.

The synthetic jarosite compositions are plotted in Figure 5 solely on the basis of their Fe^{3+} *versus* Pb^{2+} formula ratios (Table 2). Note that although all samples have Fe^{3+} less than 3, several have nil or inadequate Cu + Zn to compensate for the Fe^{3+} deficiency. The consistent presence of the deficit and, in some cases, its large size, are indications that jarosite can depart significantly from the simple ideal stoichiometry. The deficit in *R*-site occupancy also has the effect of moving some of the synthetic jarosite compositions out of the field shown in Figure 5; corrections to the cell dimensions are thus necessary to return these samples to the plane of full occupancy in the *R* position.

Figure 9a shows the *a* dimensions of end-member plumbojarosite (Mumme & Scott 1966), synthetic hydronium jarosite (Brophy & Sheridan 1965, Mumme & Scott 1966), and beaverite (average from the Caribou and Katanga specimens, Table 1). Also shown are the variations expected for ideal solid solutions, and the measured values obtained from the samples of synthetic jarosite studied here; the last are

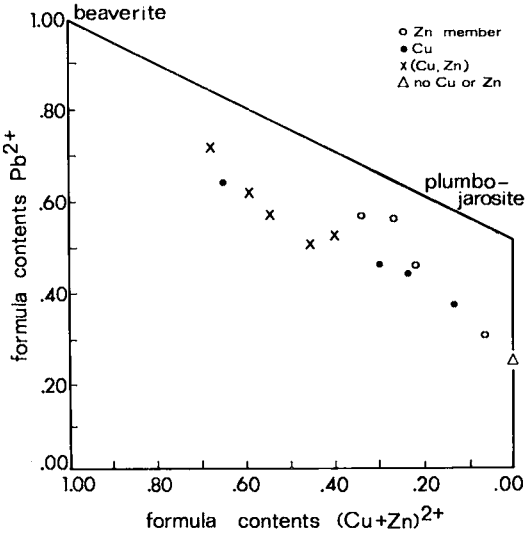

FIG. 6. Formula contents Pb^{2+} *versus* $(Cu + Zn)^{2+}$ in synthetic jarosite compositions.

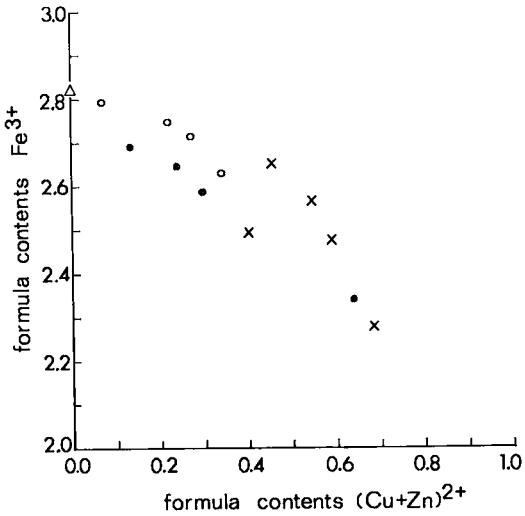

FIG. 7. Formula contents Fe^{3+} *versus* $(Cu + Zn)^{2+}$ in synthetic jarosite compositions. Symbols as in Figure 6.

positioned according to the Pb:Fe formula ratios as in Figure 5. Only three of the synthetic jarosite samples have full *R*-site occupancy (J309 to J311, Table 2). In these three, the adjustment of *a* values in order to compensate for the expansion caused by Zn^{2+} does not significantly shift *a*. A deficiency in *R*-site occupancy is characteristic of all of the remaining synthetic jarosite compositions. Among these, the three

TABLE 3. REPRESENTATIVE X-RAY POWDER PATTERN OF SYNTHETIC FERRIAN BEAVERITE (J335)

I_{est}	d_{meas}(Å)	d_{calc}(Å)	*hkl*	I_{est}	d_{meas}(Å)	d_{calc}(Å)	*hkl*
<½	11.6	11.3	003	<½	2.098	2.101	030
8	5.91	5.91	012	½	2.075	2.078	128
<½	5.65	5.67	006	4	1.968	1.970	036*
½	4.60	4.62	015	1	1.950	1.951	2.1.10*
4	3.63	3.64	110	<½	1.924	1.924	2.0.14
1	3.52	3.52	018*	4	1.816	1.820	220*
10	3.08	3.10	202	1	1.764	1.762	0.2.16
	3.06	3.06	116	½	1.737	1.732	226*
<½	2.991	2.993	1.0.10	1	1.704	1.701	1.2.14
3	2.952	2.955	024*	1	1.684	1.688	0.3.12
3	2.840	2.834	0.0.12*		1.680	1.677	1.1.18
3	2.529	2.532	208*	½	1.645	1.645	137
2	2.354	2.359	122*	1	1.554	1.555	1.3.10
<½	2.318	2.312	0.2.10		1.549	1.549	404
2	2.289	2.294	214	2	1.532	1.531	2.2.12*
5	2.269	2.267	0.1.14*	2	1.500	1.501	1.0.22*
1	2.237	2.236	1.1.12	1	1.478	1.478	048*

114.6 mm Debye-Scherrer camera; $CoK\alpha_1$ radiation (λ = 1.7889Å); intensities estimated visually; indexed with *a* 7.278, *c* 34.01Å; lines with an asterisk were used for the least-squares refinement.

samples richest in zinc have high *a* values, whereas the others have low *a* values (Fig. 9a). One sample contains neither copper nor zinc, and thus the inference is that the full *versus* partial occupancy of *R* sites must have a significant influence on the length of *a*.

Plumbojarosite D2091 has *a* 7.319 Å but plots approximately on the isopleth for 7.330 Å (Fig. 9a). The *R*-site occupancy of D2091 is 2.825 rather than 3.000 formula units, and therefore the tentative assumption is that the 0.175 deficit in Fe^{3+} has contracted *a* by 0.011 Å (0.00063 Å per 0.01 Fe^{3+}). For zincian members, two additional adjustments are required: (a) compensation for the enlarging effect of Zn^{2+}, and (b) compensation for the fact that adjustment (a) merely "neutralizes" Zn and, therefore, the R^{3+} deficit is the sum of Zn plus the Fe^{3+} shortage.

Calculated *a* values of the *R*-deficient jarosite samples were obtained using $a(\text{calc}) = a(\text{meas}) + 0.063(Fe\bigstar + Zn) - 0.0258$ Zn, where Fe★ is the Fe^{3+} deficit and Zn is the formula content of Zn. The reasonably good agreement among the calculated *a* values and the *a*-dimension isopleths in Figure 9b demonstrates that the length of *a* seems to be governed principally by the proportion of Cu, Fe and Zn and the total number of ions in the *R* sites. The regression equation for calculated *a* versus (Cu + Zn) is a (Å) = 7.326 − 0.080 (Cu + Zn), with a standard deviation in *a* of 0.0034 Å. A similar variation occurs with Pb^{2+}, but the greater scatter of the data points suggests that the trend is present mainly because of the pairing of *A*- and *R*-site divalent ions, as shown in Figure 6.

Although the *A*-site ions are generally thought to have little effect on *a*, they are theoretically responsible for the main variations in *c*. Figure 9c shows the standard triangular diagram and *c*

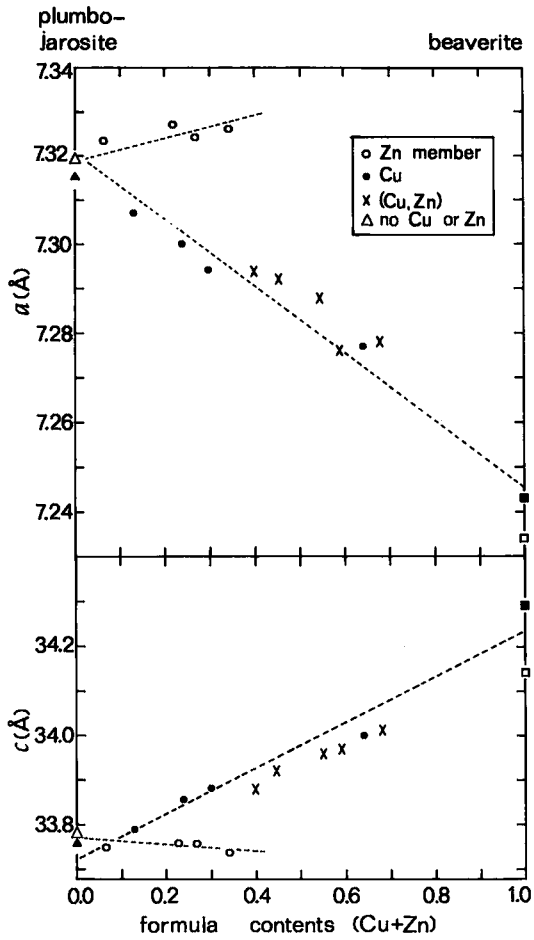

FIG. 8. Variations in *a* and *c* related to composition changes in synthetic jarosite. End members are natural plumbojarosite (solid triangle; after Mumme & Scott 1966), synthetic plumbojarosite (open triangle; sample D2091 in Table 2), beaverite from the Caribou deposit (open square) and Katanga (solid square).

values for plumbojarosite, beaverite and hydronium jarosite end-members. The roles that the various cations play in governing *c* can be determined in the same way as was done for *a:* along the plumbojarosite – hydronium jarosite join, the change in *c* is −0.0262 Å per 0.1 formula unit H_3O that is lost as plumbojarosite is approached. The horizontal dashed line from plumbojarosite (Fig. 9c). extends to $Pb_{0.5}(H_3O)_{0.5}(Cu_{0.5}Fe_{2.5})(SO_4)_2(OH)_6$, with *c* 34.17 Å. The amount of increase in *c* that is attributable to H_3O is 5 × 0.0262 Å, leaving 0.281 Å attributable to Cu^{2+} replacement of Fe^{3+} (0.281/0.5 Cu = 0.0562 Å per 0.1 Cu).

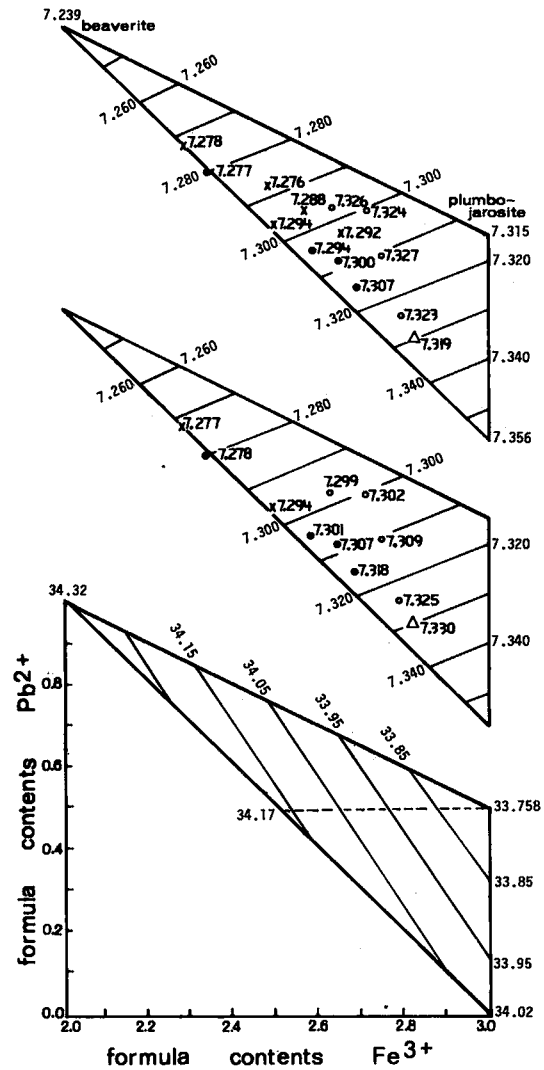

FIG. 9. Same reference points and symbols as shown in Figure 5 (beaverite–plumbojarosite–hydronium jarosite). *Figure 9a* (top) shows variations in *a* for assumed solid solutions among the end members, and the measured *a* values of the synthetic jarosites. *Figure 9b* (middle) shows the improved correlation for *R-deficient* jarosites after measured *a* values have been corrected for Zn^{2+} content and Fe^{3+} deficiences. *Figure 9c* (bottom) shows the varition in *c* for assumed solid solutions among the end members.

Along the plumbojarosite – beaverite join the increase in *c* is related to (Cu, Fe) solid solution and to the Pb content, which increases from 0.5 in plumbojarosite to 1.0 in beaverite. The increase due to Cu^{2+} substitution is known from above to be 0.0562 Å per 0.1 Cu; thus, the effect of

increasing the Pb formula content from 0.5 to 1.0 is: $33.758_p + 0.562_{Cu}$ (where p is c of plumbojarosite, and Cu is the increase attributed to Cu). The sum of these is 34.32, identical to the c axis of beaverite; the inference from this unexpected result thus is that the amount of Pb in A sites has a negligible effect on the length of c.

Figure 8 shows that the replacement of Fe^{3+} by Zn^{2+} has little influence on the length of c, and that the dominant control is the amount of Cu^{2+} in the series. Therefore, subtraction of Zn from the formula contents of the copper-bearing jarosite compositions shown in Figure 8 gives a more precise relationship, for which the regression equation is: c (Å) = 33.715 + 0.533 Cu; the standard deviation in c is 0.0437.

The apparent lack of response of c to Pb^{2+} content may arise simply because additional Pb^{2+} ions can be accommodated in existing A-site vacancies without disturbing the structure. In plumbojarosite only half the available A sites are filled, but the synthetic jarosite compositions show that the structure readily tolerates additional Pb^{2+}, $(H_3O)^+$, or additional vacancies. Indications from the chemical analyses and X-ray patterns are that less than a third of the A sites need to be filled by Pb^{2+} to attain a 34 Å c axis (sample D2090, Table 2). That hydronium ion has occupied some of the A sites to provide additional support for the structure is a possibility that cannot be discounted because the chemical and thermogravimetric data show that the majority of jarosite samples have excess H_2O. Although the larger radius of $(H_3O)^+$ (r = 1.24 Å) relative to Pb^{2+} (r = 1.12 Å) should expand c, anomalous c values apparently are not present (radii according to Kubisz 1964).

Powder-Diffraction Features

Synthetic jarosite

Although the doubled (~34 Å) c axis that characterizes plumbojarosite was used in this study, in general appearance the X-ray powder patterns of the samples of synthetic jarosite are similar to that of beaverite (c ~17 Å). For example, it is evident from the indices assigned in Table 3 that only a few diffraction lines of very weak intensity necessitate the doubling of c. In general, the first two lines in the powder pattern of plumbojarosite are the most definitive indications of a plumbojarosite cell: d 11:27 Å (003) with intensity 13, and d 6.232 Å (101) with intensity 34 (Mumme & Scott 1966). However, the synthetic jarosite compositions studied here have (101) extremely weak or absent, and it is this major difference that gives the X-ray patterns their beaverite appearance. Despite the (101) disappearance, the 11 Å line is more persistent and has been observed for several of the synthetic jarosite compositions. Experience has shown that the most reliable method of detecting the 11 Å line is to use Debye–Scherrer cameras of 114.6-mm diameter, and radiation with a wavelength longer than that of copper. Cobalt radiation (λ = 1.7889 Å) has been used throughout this study because it provides suitable wavelength and intensity characteristics.

The current consensus is that all members of the alunite – jarosite group, other than plumbojarosite and minamiite, have a 17 Å c axis. The existence of solid-solution series between beaverite and plumbojarosite, and between plumbojarosite and hydronium jarosite, thus require transformations from 17 Å to 34 Å c axes. Mumme & Scott (1966) studied the series hydronium jarosite – plumbojarosite and were unable to detect the transformation even though their series extended up to 88.7 mol. % plumbojarosite. Therefore, they suggested that the plumbojarosite cell requires a high degree of order and thus forms only when the lead content closely approaches that of the ideal formula.

Table 2 summarizes the results obtained from a careful inspection for the 11 Å diffraction line in the jarosite samples studied here. Despite the uncertainty that arises because of the faint intensity of the 11 Å line in some of the X-ray patterns, others in the series (Table 2) show that an enlarged jarosite cell is present over a considerable range in composition. Thus a specific lead content is not necessary to form the enlarged cell; on the contrary, the presence or absence of the 11 Å line does not seem to be predictable from the bulk composition of a jarosite sample.

Aging and heating experiments

Infrared absorption studies and low-temperature heating experiments indicate that the synthetic jarosite samples retain about 0.5 wt. % adsorbed water despite drying at 110°C prior to chemical analysis. During a search for the 11 Å diffraction line among samples of alkali-rich synthetic jarosite, it also was noted that one sample had undergone a minor change in cell dimensions after a year of aging in a sealed bottle. Therefore, to check the stability of the samples of synthetic jarosite, three lead-rich samples were examined in more detail; two of these are D2091 and D2090 (Table 2), and the other is roughly similar in composition to D2091

but had been precipitated and X-rayed about 6 months earlier.

X-ray powder-diffraction films had been taken of all three samples after heating each to 110°C for about 24 hours. Additional X-ray films were taken after heating to 110°C for 14 days, 150°C for 24 hours, and 190°C for 24 hours. All samples showed negligible changes in cell dimensions and diffraction intensities or sharpness.

Natural jarosite

Examination of other samples of synthetic jarosite, including those with only monovalent ions in *A* sites, revealed that the presence of the 11 Å diffraction line is not a rare phenomenon. A similar check of about 15 specimens of natural jarosite showed that, in most cases, this line is either absent or indistinct, but a few do have the 11 Å line even though their compositions indicate that the *c*-axis length should be ~17 Å. The best example, with a medium-intensity 11 Å line, is jarosite from the Darwin mine, California (Table 4). Although the specimen is fine grained, it may eventually provide a grain suitable for a crystal-structure determination. X-ray precession studies to date have revealed that the mineral is strongly pseudo-hexagonal, but the true symmetry is orthorhombic, and the *c* axis is ~34 Å (J.T. Szymański, oral comm. 1982). This result might not only explain the "anomalous" occurrence of the 11 Å powder-diffraction line, but might also account for several reports of optically biaxial jarosite (Palache *et al.* 1951).

In other samples, however, the 11 Å line may be a reflection of a normal 34 Å hexagonal cell. For example, in the new mineral *minamiite*, $(Na_{0.36}K_{0.1}Ca_{0.27}\square_{0.27})Al_3(SO_4)_2(OH)_6$, bond lengths indicate that the *A* sites can be divided in two sets, each with different cation-populations; the 34 Å *c* axis arises because of partial ordering of cations in each set (Ossaka *et al.* 1982). A structural model of this type would permit the enlarged cell to occur over a very wide composition field, exactly as has been found in the present study.

The occurrence of minamiite also demonstrates that only partial occupancy of the *A* sites need occur; this variability is in contrast to the interpretation of most analyses in which exactly half of the *A* sites are assumed to be occupied, as in stoichiometric plumbojarosite, or else complete occupancy is assumed by addition of hydronium. Although nothing is known of the structural effects of *R*-site vacancies, it should be noted that any ordered arrangement of vacancies in *R* will have the effect of removing jarosite from its usual space group, $R\bar{3}m$.

Published jarosite analyses that deviate significantly from stoichiometric proportions are so few as to be disturbing, and it seems likely that some results may have been misinterpreted as unsatisfactory analyses or analyses of mixtures. That there is a need for caution in interpreting chemical data for bulk samples of fine-grained jarosite is evident from the severe compositional zoning detected in a specimen labelled argentojarosite from the Tintic Standard mine, Dividend, Utah (Fig. 10). Crystals of this material consist of a core of (K) jarosite, intermediate zones of plumbojarosite and a broad rim of natrojarosite (Table 4).

The extent of cation variations possible in natural jarosite-group minerals is illustrated by the plumbian, cuprian alunite described by Cortelezzi (1977). The recalculated composition of the mineral is $(K_{0.61}Pb_{0.34}Na_{0.11})_{\Sigma 1.06}(Cu_{0.51}Zn_{0.04}Fe_{0.20}Al_{1.63})_{\Sigma 2.38}(SO_4)_2(OH)_{5.65}$; the (OH) formula requirements for charge balance are 3.99. Aside from the cation variations, a notable feature of this alunite is the large deficiency in the *R* site. The powder pattern of the mineral as given by Cortelezzi (1977) has several indices forbidden by the standard ($R\bar{3}m$) alunite cell.

TABLE 4. RESULTS OF MICROPROBE ANALYSES OF JAROSITE

	Darwin mine, Inyo Co. California		Tintic Standard mine, Dividend Utah (Figure 11)		
	1	2	core	intermed.	main rim
wt.% Na_2O	0.0	0.0	0.0	0.0	7.0
K_2O	9.0	9.2	8.2	0.1	0.0
PbO	-	-	2.4	16.8	0.0
Fe_2O_3	46.3	46.9	45.8	41.8	48.9
SO_3	32.5	32.5	31.7	28.7	33.2
	87.8	88.6	88.1	87.4	89.1
(H_2O)*	12.2	11.4	11.9	12.6	10.9
			ratios for SO_4 = 2		
Na	0.00	0.00	0.00	0.00	1.09
K	0.95	0.96	0.88	0.01	0.00
Pb	-	-	0.05	0.42	0.00
Fe	2.86	2.90	2.89	2.92	2.95
SO_4	2.00	2.00	2.00	2.00	2.00
OH	6.68	6.18	6.72	7.86	5.88

Analyses by T.T. Chen (Darwin mine) and D.R. Owens.

* H_2O by difference from 100 wt. %.

Conclusions

1. Extensive substitution of divalent ions for Fe^{3+} has been demonstrated for synthetic plumbojarosite; as the amounts of Cu^{2+} and Zn^{2+} increase, Fe^{3+} decreases (Fig. 7). A complete compositional series probably extends from plumbojarosite to beaverite.
2. For the above compositions of jarosite, the *a* cell dimension is controlled principally by

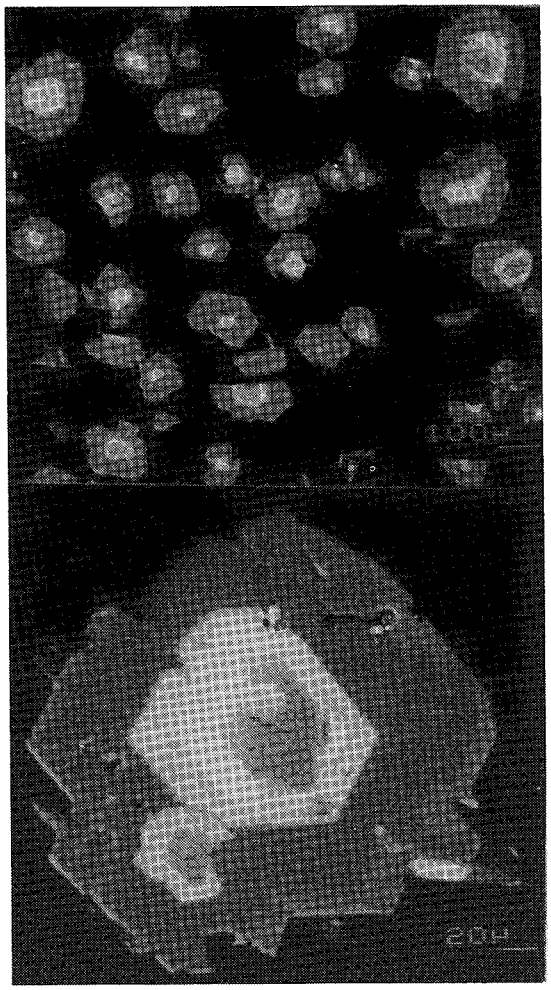

FIG. 10. Jarosite from Tintic Standard mine, Dividend, Utah. Top back-scattered electron image shows that zoning is present in all complete grains, and bottom image shows the compositional complexity in individual particles. Representative analyses of the main zones are given in Table 4; white zones are Pb-rich.

the proportions of Cu, Zn and Fe and the total number of ions in the *R* sites. Variations in *c* are related mainly to the amount of Cu^{2+} that has replaced Fe^{3+}.

3. Chemical analyses indicate that many of the synthetic jarosite compositions are deficient in metals that occupy the *R* sites. The frequent occurrence of this deficiency, and in some cases the largeness of the deficit, strongly suggest that nonstoichiometry is a characteristic trait of some jarosite-group minerals. The fact that such deficiencies affect the *a* cell dimension, and especially that a quantitative relationship is demonstrable, is compelling evidence of non-stoichiometry.

4. There is a need to determine the nature of pseudohexagonal jarosite, to examine additional samples of jarosite for an 11 Å diffraction line and ascertain the specific reason for its presence, to establish the extent of *A*- and *R*-site vacancies tolerated in jarosite and to correlate structural effects of partial occupancy of cation sites. Current crystallochemical concepts about the jarosite group require considerable broadening to account for these phenomena.

ACKNOWLEDGEMENTS

The microprobe analyses were done by T.T. Chen and D.R. Owens, polished and thin sections were prepared by J.H.G. Laflamme and J.M. Beaulne, and assistance with the X-ray powder studies was given by E.J. Murray and P.E. Bélanger. Single-crystal Xray examination of the samples of natural jarosite was done by J.T. Szymanski. O. Dinardo helped to prepare the synthetic jarosite samples. Several jarosite specimens were obtained from the National Mineral Collection, Ottawa through the courtesy of H.G. Ansell, from the Royal Ontario Museum *via* J.A. Mandarino, and from the British Museum (Natural History) through the efforts of J.P. Fuller.

REFERENCES

BOLGOV, G.P. (1956): Beaverite and its paragenesis in the zone of oxidation of sulfide deposits. *Akad. Nauk Kazakh. SSR, Izv. Ser. Geol.* **23**, 63-73 (in Russ.)

BOLTON, G.L., ZUBRYCKYJ, N. & VELTMAN, H. (1979): Pressure leaching process for complex zinc–lead concentrates. *Int. Mineral Process. Congr. (13th) Proc.* **1**, 583-607.

BROPHY, G.P., SCOTT, E.S. & SNELLGROVE, R.A. (1962): Sulfate studies. II. Solid solution between alunite and jarosite. *Amer. Mineral.* **47**, 112-126.

——— & SHERIDAN, M.F. (1965): Sulfate studies IV. The jarosite – natrojarosite – hydronium jarosite solid solution series. *Amer. Mineral.* **50**, 1595-1607.

BUTLER, B.S. & SCHALLER, W.T. (1911): Some minerals from Beaver County, Utah. *Amer. J. Sci.* **182**, 418-424.

CORTELEZZI, C.R. (1977): Occurrence of osarizawaite in Argentina. *Neues Jahrb. Mineral. Monatsh.*, 39-44.

DUTRIZAC, J.E. & DINARDO, O. (1982): The co-precipitation of copper and zinc with lead jarosite. *CANMET Div. Rep. MRP/MSL* **82–88**, *Can. Dep. Energy, Mines Res.*

———, ——— & KAIMAN, S. (1980): Factors affecting lead jarosite formation. *Hydrometall.* **5**, 305-324.

——— & KAIMAN, S. (1976): Synthesis and properties of jarosite-type compounds. *Can. Mineral.* **14**, 151-158.

ENIKEEV, M.R. (1964): Beaverite from Altyn–Topkan. *Nauchn. Tr., Tashkentsk. Gos. Univ.* **249**, 36-39 (in Russ.).

GIUSEPPETTI, G. & TADINI, C. (1980): The crystal structure of osarizawaite. *Neues Jahrb. Mineral. Monatsh.*, 401-407.

HENDRICKS, S.B. (1937): The crystal structure of alunite and the jarosites. *Amer. Mineral.* **22**, 773-784.

JAMBOR, J.L. (1981): Mineralogy of the Caribou massive sulphide deposit, Bathurst area, New Brunswick. *CANMET Rep.* **81–8E**, *Can. Dep. Energy Mines Res.*

KATO, T. (1979): The crystal structure of plumbojarosite. *Mineral. Soc. Japan Ann. Meet.*, 26 (abstr.; in Jap.).

——— & MIURA, Y. (1977): The crystal structures of jarosite and svanbergite. *Mineral. J. (Japan)* **8**, 419-430.

KUBISZ, J. (1964): A study on minerals of the alunite–jarosite group. *Polska Akad. Nauk Prace Geol.* **22**, 1-85 (in Polish).

——— (1970): Studies on synthetic alkali-hydronium jarosites. I. Synthesis of jarosite and natrojarosite. *Mineral. Polonica* **1**, 47-57.

LECLERC, A. (1980): Room temperature Mössbauer analysis of jarosite-type compounds. *Phys. Chem. Minerals* **6**, 327-334.

MENCHETTI, S. & SABELLI, C. (1976): Crystal chemistry of the alunite series: crystal structure refinement of alunite and synthetic jarosite. *Neues Jahrb. Mineral. Monatsh.*, 406-417.

MORRIS, R.C. (1962): Osarizawaite from Western Australia. *Amer. Mineral.* **47**, 1079-1093.

——— (1963): Osarizawaite from Western Australia – a correction. *Amer. Mineral.* **48**, 947.

MUMME, W.G. & SCOTT, T.R. (1966): The relationship between basic ferric sulfate and plumbojarosite. *Amer. Mineral.* **51**, 443-453.

OSSAKA, J., HIRABAYASHI, J., OKADA, K., KOBAYASHI, R. & HAYASHI, T. (1982): Crystal structure of minamiite, a new mineral of the alunite group. *Amer. Mineral.* **67**, 114-119.

PALACHE, C., BERMAN, H. & FRONDEL, C. (1951): *The System of Mineralogy*. 2. *(7th ed.)* John Wiley & Sons, New York.

SCOTT, T.R. (1973): Continuous co-current pressure leaching of zinc–lead concentrates under acid conditions. *In* International Symposium on Hydrometallurgy (D.J.I. Evans & R.S. Shoemaker, eds.). American Institute Mining Metallurgical Engineers, New York.

TAGUCHI, Y. (1961): On osarizawaite, a new mineral of the alunite group, from the Osarizawa mine, Japan. *Mineral. J. (Japan)* **3**, 181-194.

———, KIZAWA, Y. & OKADA, N. (1972): On beaverite from the Osarizawa mine. *Kobutsugaku Zasshi* **10**, 313-325 (in Jap.).

VAN TASSEL, R. (1958): Jarosite, natrojarosite, beaverite, léonhardtite et hexahydrite du Congo belge *Inst. roy. Sci. nat. Belg. Bull.* **34**, 1-12.

VITOVSKAYA, I.V. (1960). New data on the mineralogy of the oxidation zone of the Akchagyl deposit in central Kazakhstan. *Kora Vyvetrivaniya, Akad. Nauk S.S.S.R., Inst. Geol. Rudnykh Mestorozhden. Petrog. Mineral. Geokhim.* **3**, 74-116 (in Russ.).

WANG, R., BRADLEY, W.F. & STEINFINK, H. (1965): The crystal structure of alunite. *Acta Cryst.* **18**, 249-252.

Received April 29, 1982, revised manuscript accepted September 15, 1982.